Supporting Material

Sodium-Calcium Exchange is Essential for Effective Triggering of Calcium Release in Mouse Heart

Patricia Neco, Beth Rose, Nhi Huynh, Rui Zhang, John H. B. Bridge, Kenneth D. Philipson, and Joshua I. Goldhaber

DETAILED METHODS

Generation of Transgenic Mice

We generated cardiac-specific NCX KO mice by ablating exon 11 of the exchanger using Cre/loxP technology. This method deletes NCX from ~80% of ventricular cardiomyocytes (1). The mice used in this study were between 8 and 12 weeks of age, did not display any gross pathology, had good cardiac function, and exhibited no evidence of heart failure.

Isolation of Ventricular Myocytes From Adult Mouse Hearts

All procedures were in accordance with the guidelines of the UCLA Office for Protection of Research Subjects. Mice weighing between 20 - 30 g were injected with 200 μl heparin (10,000 units/ml) i.p. 20 minutes before explantation of the hearts. Animals were anesthetized with isoflurane and hearts quickly excised via thoracotomy. Isolation of ventricular myocytes by collagenase/protease digestion was performed using the method we have described previously (2). Following isolation, we stored the dissociated cells for up to 6 hours at room temperature in modified Tyrode's solution, containing (in mmol/L): 136 NaCl, 5.4 KCl, 10 HEPES, 1.0 $MgCl_2$, 0.33 NaH_2PO_4, 0.5 $CaCl_2$, 10 glucose, (pH 7.4). This solution, with additional modifications described below, was also used as the standard bath for electrophysiological recordings.

Electrophysiology

We placed isolated myocytes in an optical chamber containing the bath solution described above. In some experiments, myocyte movements were arrested by the temporary addition of 10 mM BDM (2,3-butanodione monoxime) to the solution for 15 min. This facilitated formation of the whole cell patch. BDM was removed before starting recordings to reverse its uncoupling effects (3-5). We used 1–2 MΩ firepolished borosilicate pipettes (World Precision Instruments, Inc., Sarasota, FL). The pipette internal solution contained (in mM): 130 KCl, 10 NaCl, 20 K-HEPES, 0.05 cAMP, 5 phosphocreatine, 5 Mg-ATP, 1 K_5Fluo-3 and either 0 or 3 EGTA. $CaCl_2$ was adjusted to obtain a free [Ca^{2+}] of 100 nM, calculated using the Maxchelator program (Webmaxclite v1.15). Fluo-3 was included to record local Ca^{2+} release events and whole cell transients as described previously (6). 5 mM reduced glutathione was included to reduce phototoxicity. All solutions had an osmolarity of ~300 mOsmols and the pH was adjusted to 7.2.

We used an Axopatch 1A amplifier (Molecular Devices, Sunnyvale, CA) in Bridge mode and the Clampex component of the pCLAMP 8.2 software suite (Molecular Devices) to pace cells and record APs. APs were elicited at 1 Hz using a 5 ms depolarizing current, ~20% above threshold. Each test AP was preceded by 10 conditioning APs at a frequency of 1 Hz.

Experiments were performed at 20-22º C. Chemicals were purchased from Sigma-Aldrich (St. Louis, MO) or Fisher (Fisher Scientific, Pittsburgh, PA); fluo-3 and di-8-ANEPPS were purchased from Invitrogen (Eugene, OR).

Measurement and Analysis of Ca^{2+} Sparks

To record Ca sparks in resting unstimulated patch clamped cells (holding potential -75 mV), we used the line scan mode (2 ms/line) of a Zeiss Pascal 5 laser scanning confocal system (Carl Zeiss, Inc., Thornwood, NY) on a Zeiss Axiovert 100 LSM inverted microscope fitted with a 63X water immersion objective (Zeiss C-Apochromat 63/1.2 W Corr). For these experiments, the patch pipette solution contained 0.1 mM fluo-3 and no EGTA. Cells were excited at 488 nm using an Argon/Krypton laser and fluorescence emission wavelengths greater than 510 nm were detected

by the photomultiplier of the confocal system. In other experiments we recorded Ca sparks in resting myocytes permeabilized with the membrane detergent saponin (0.01% for 60 s; 7). After permeabilization, cells were placed in a mock intracellular solution for imaging, containing (in mM): K-aspartate 120; KCL 20; KH_2PO_4 1, KADP 1; NaPyruvate 2; EGTA 1; $CaCl_2$ 0.27; $MgCl_2$ 1.13; HEPES 20; K_5Fluo-4 0.06; creatine 1; glucose 2; dextran (MW: 40,000) 8%, and pH 7.2. Free Ca^{2+} and Mg^{2+} of this solution were 60 nm and 0.67 mM respectively. In additional experiments we adjusted free Ca to 100 nM.

To record Ca^{2+} sparks evoked by APs, we used the rapid line scan mode (0.24 ms/line) of a Noran Odyssey XL laser scanning confocal system (Noran Instruments, Middleton, WI, USA) attached to a Zeiss Axiovert TV100 inverted microscope fitted with a 40X water immersion objective lens (Zeiss C-Apochromat 40/1.2 W Corr). Image acquisition was electronically synchronized with APs by using the Noran's Silicon Graphics Indy (Silicon Graphics, Inc., Mountain View, CA) workstation to trigger Clampex on the patch clamp computer. Synchronization was verified by flashing a light emitting diode. Pixel resolution was 0.19 μm. To reduce photobleaching of the indicator as well as phototoxicity to the cells, the laser was shuttered electronically and triggered to open only during the 230 ms acquisition period.

Fluorescence transients were normalized as $\Delta F/F = (F - F_o)/F_o$ and characterized by their amplitude $(\Delta F/F)_{peak}$ and latency. These parameters were calculated on filtered images (3 space pixels, 11 time pixels) with a computer-assisted method under the IDL™ (ITT Visual Information Solutions, Boulder, CO) structured language (6). This program also identifies the onset of individual Ca sparks during high speed confocal imaging, so that they can be counted, as described previously (6). Latency was defined as the period between the AP stimulus and the point at which the spark fluorescence rose 10% above baseline (6). Since the cell occupies the entire scan line, whose length is a fixed value in the Noran confocal, spark numbers can be compared between cells and conditions without normalizing to an arbitrary length. Background fluorescence was undetectable in non-cellular areas. Identification of resting sparks was based on the threshold algorithm described by Cheng et al. (8).

Measurement of di-8-ANEPPS t-tubule Fluorescence.

To visualize the t-tubular network, cells were incubated with 10 μM di-8-ANEPPS for 10 min at room temperature, followed by 10 min of washout. Fluorescence profiles of these data were obtained by plotting fluorescence intensity vs. pixel position. Sarcomere lengths were estimated from Gaussian fits to fluorescence profiles obtained from background subtracted images. T-tubule densities were estimated by calculating the percentage of pixels within each cell that are positive for di-8-ANEPPS staining with respect to the total amount of pixels in the cell (9). Background subtracted thresholded images were used for this purpose.

Determination of Cellular Phenotype.

About twenty percent of myocytes isolated from KO hearts have a WT phenotype (1). Since NCX currents cannot be elicited reliably by caffeine in cells dialyzed with high concentrations of EGTA (10), we relied upon the characteristic differences in AP shape (11) to identify and exclude WT cells in those experiments where the internal solution contained 3 mM EGTA. In all other experiments, we tested for NCX current by rapid application of 5 mM caffeine to release internal Ca^{2+} stores. We excluded cells from the KO group if they exhibited NCX current.

Statistics

Values are presented as Mean ± S.E.M. We used Student's *t*-test to establish significant differences ($P < 0.05$) between groups.

FIGURE S1

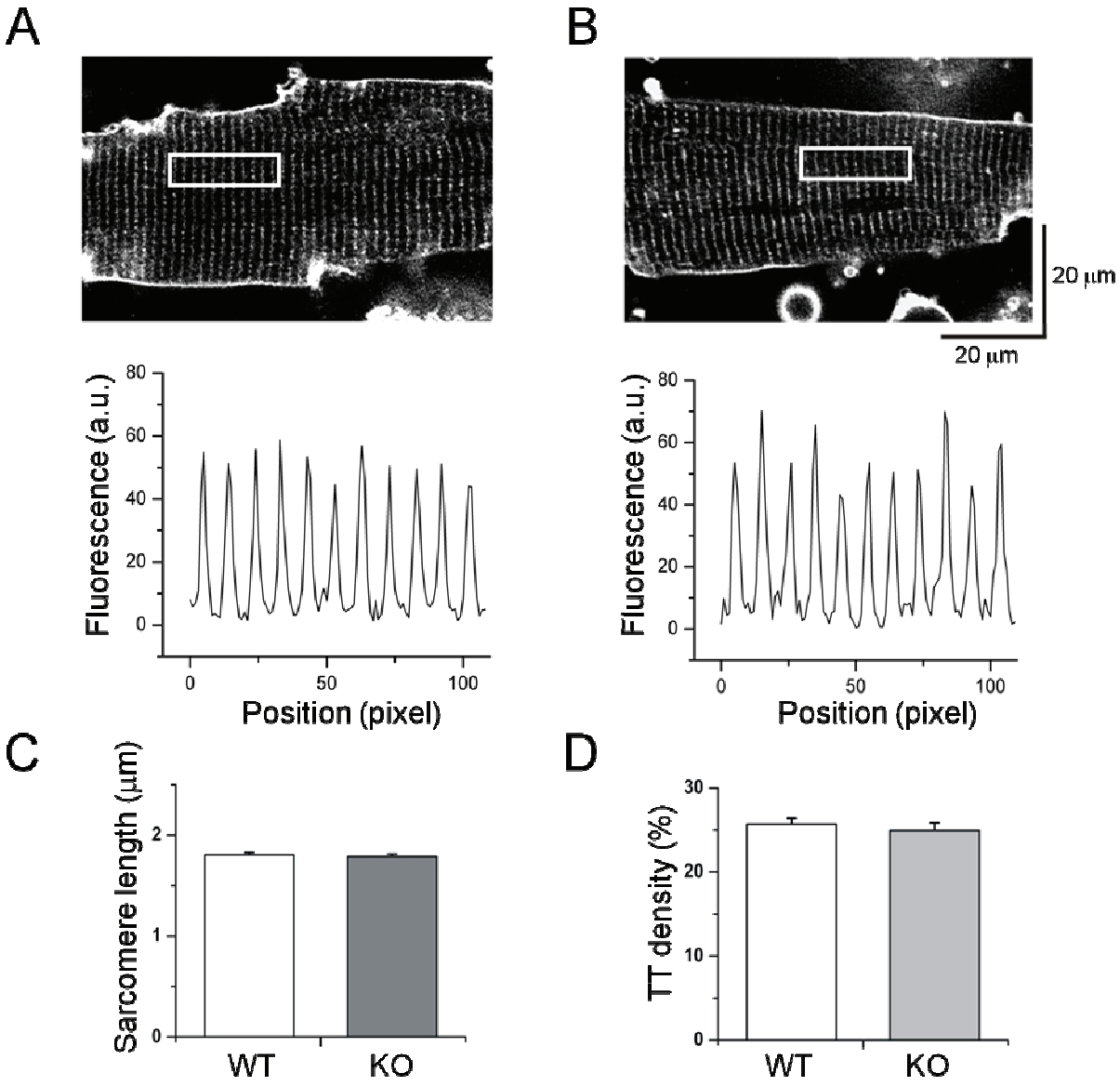

Figure 1-S. T-tubule network in NCX KO ventricular myocytes.
Confocal 2D image of a segment of representative WT (A) and KO (B) myocytes whose membranes were loaded with the potentiometric dye di-8-ANEPPS. The lower panels in A and B plot the fluorescence intensity profiles vs. the pixel position of the regions of interest indicated in the respective upper panel by the white outline. Images were 410 x 245 pixels and the acquisition time was 260 ms. They were processed to yield the optimal contrast by adjusting the background intensity level to zero and the maximal intensity to saturation. Bar plots showing the averaged sarcomere length (C) and T-tubule (TT) density (D) calculated from di-8-ANEPPS confocal

images recorded in WT (N =7) and KO (N =10) myocytes. There was no significant difference in WT vs. KO.

BIBLIOGRAPHY FOR SUPPORTING MATERIAL

1. Henderson, S. A., J. I. Goldhaber, J. M. So, T. Han, C. Motter, A. Ngo, C. Chantawansri, M. R. Ritter, M. Friedlander, D. A. Nicoll, J. S. Frank, M. C. Jordan, K. P. Roos, R. S. Ross, and K. D. Philipson. (2004). Functional adult myocardium in the absence of Na^+-Ca^{2+} exchange: cardiac-specific knockout of NCX1. Circ Res *95*, 604-611.
2. Reuter, H., T. Han, C. Motter, K. D. Philipson, and J. I. Goldhaber. (2004). Mice overexpressing the cardiac sodium-calcium exchanger: defects in excitation-contraction coupling. J Physiol *554*, 779-789.
3. Brotto MA, F. R., Creazzo TL, Godt RE, Nosek TM. (1994). The effect of 2,3-butanedione 2-monoxime (BDM) on ventricular trabeculae from the avian heart. J Muscle Res Cell Motil. *16*, 1-10.
4. Cheng Y, M. K., Efimov IR, Van Wagoner DR, Tchou PJ, Mazgalev TN. (1997). Effects of 2,3-butanedione monoxime on atrial-atrioventricular nodal conduction in isolated rabbit heart. J Cardiovasc Electrophysiol. *8*, 790-802.
5. Nakayama Y, K. K. K., Yoneyama M and Hachiro T. (2005). Rhythmic contraction and intracellular Ca2+ oscillatory rhythm in spontaneously beating cultured cardiac myocytes. Biological Rhythm Research *36*, 315 - 324.
6. Chantawansri, C., N. Huynh, J. Yamanaka, A. Garfinkel, S. T. Lamp, M. Inoue, J. H. Bridge, and J. I. Goldhaber. (2008). Effect of metabolic inhibition on couplon behavior in rabbit ventricular myocytes. Biophys J *94*, 1656-1666.
7. Zima, A. V., J. Kockskamper, and L. A. Blatter. (2006). Cytosolic energy reserves determine the effect of glycolytic sugar phosphates on sarcoplasmic reticulum Ca2+ release in cat ventricular myocytes. J Physiol *577*, 281-293.
8. Cheng, H., L. S. Song, N. Shirokova, A. González, E. G. Lakatta, E. Ríos, and M. D. Stern. (1999). Amplitude distribution of calcium sparks in confocal images: theory and studies with an automatic detection method. Biophys J *76*, 606-617.
9. He, J., M. W. Conklin, J. D. Foell, M. R. Wolff, R. A. Haworth, R. Coronado, and T. J. Kamp. (2001). Reduction in density of transverse tubules and L-type Ca^{2+} channels in canine tachycardia-induced heart failure. Cardiovasc Res *49*, 298-307.
10. Adachi-Akahane, S., L. Cleemann, and M. Morad. (1996). Cross-signaling between L-type Ca2+ channels and ryanodine receptors in rat ventricular myocytes. J Gen Physiol *108*, 435-454.
11. Pott, C., X. Ren, D. X. Tran, M. J. Yang, S. Henderson, M. C. Jordan, K. P. Roos, A. Garfinkel, K. D. Philipson, and J. I. Goldhaber. (2007). Mechanism of shortened action potential duration in Na+-Ca2+ exchanger knockout mice. Am J Physiol Cell Physiol *292*, C968-973.